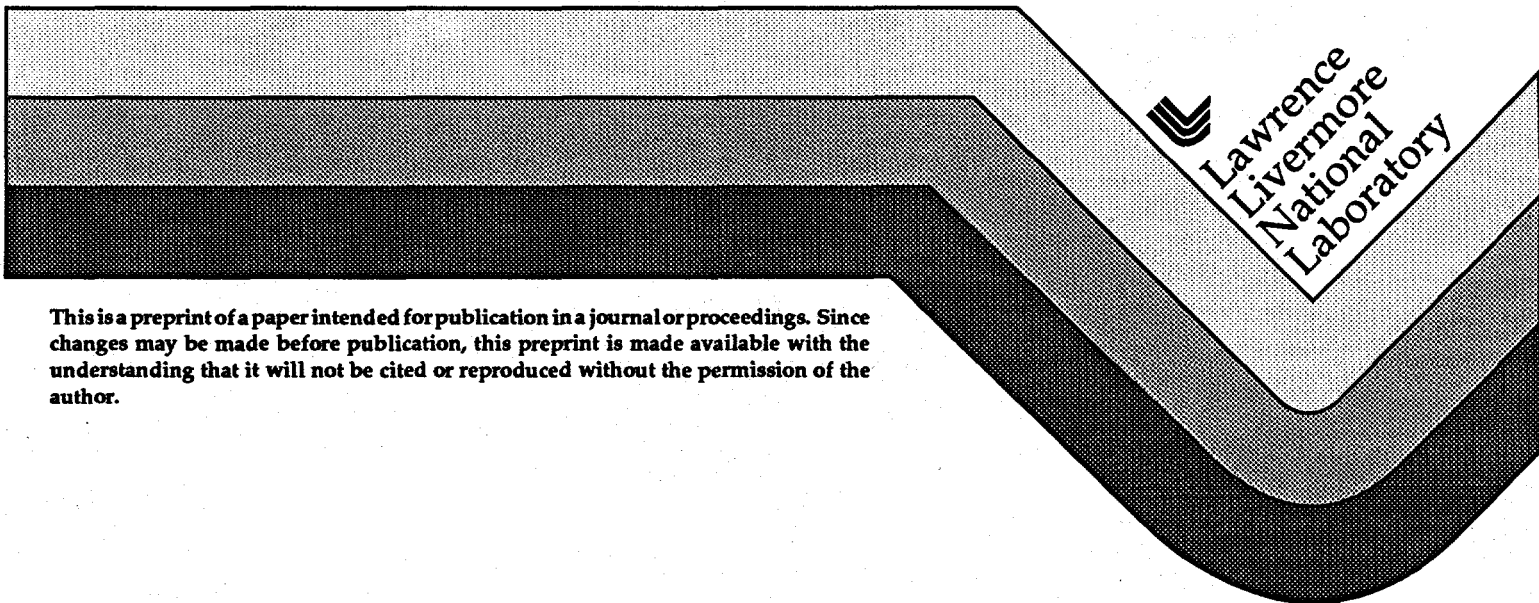


**Scalar Wave Diffraction  
from a Circular Aperture**

**C. Cerjan**

**This paper was prepared for submittal to the  
Extreme Ultraviolet Lithography Topical Meeting  
Monterey, CA  
September 19-21, 1994**

**January 25, 1995**



**Lawrence  
Livermore  
National  
Laboratory**

**This is a preprint of a paper intended for publication in a journal or proceedings. Since changes may be made before publication, this preprint is made available with the understanding that it will not be cited or reproduced without the permission of the author.**

**UG DISTRIBUTION OF THIS DOCUMENT IS UNLIMITED**

#### DISCLAIMER

This document was prepared as an account of work sponsored by an agency of the United States Government. Neither the United States Government nor the University of California nor any of their employees, makes any warranty, express or implied, or assumes any legal liability or responsibility for the accuracy, completeness, or usefulness of any information, apparatus, product, or process disclosed, or represents that its use would not infringe privately owned rights. Reference herein to any specific commercial product, process, or service by trade name, trademark, manufacturer, or otherwise, does not necessarily constitute or imply its endorsement, recommendation, or favoring by the United States Government or the University of California. The views and opinions of authors expressed herein do not necessarily state or reflect those of the United States Government or the University of California, and shall not be used for advertising or product endorsement purposes.

## **DISCLAIMER**

**Portions of this document may be illegible in electronic image products. Images are produced from the best available original document.**

# Scalar Wave Diffraction from a Circular Aperture

C. Cerjan  
Advanced Microtechnology Program  
Lawrence Livermore National Laboratory  
Livermore, CA 94550

## Abstract

The scalar wave theory is used to evaluate the expected diffraction patterns from a circular aperture. The standard far-field Kirchhoff approximation is compared to the exact result expressed in terms of oblate spheroidal harmonics. Deviations from an expanding spherical wave are calculated for both cases as a function of the circular aperture radius and the incident beam wavelength using suggested values for a recently proposed point diffraction interferometer. The Kirchhoff approximation is increasingly reliable in the far-field limit as the aperture radius is increased, although significant errors in amplitude and phase persist.

## 1. Motivation

Although the problem of single mode, plane scalar wave diffraction through a circular aperture is often presented in elementary textbooks [1], this treatment is usually limited to the large aperture far-field limit. Besides neglecting the vectorial nature of the electromagnetic wave, the Kirchhoff approximation to the solution of the full integral equation for the scattered wave is used which is widely known to be mathematically inconsistent [2]. The outstanding difficulty is thus determining the reliability of the

 DISTRIBUTION OF THIS DOCUMENT IS UNLIMITED

**MASTER**

standard treatment, especially if high accuracy is necessary.

An exact treatment of scalar plane wave diffraction from a circular aperture exists [3],[4]. Since it requires the numerical evaluation of the oblate spheroidal angular and radial functions, this theory is not widely applied. For the precise, high resolution metrology envisioned for a recently suggested Point Diffraction Interferometer (PDI)[5], it seems prudent to develop this exact approach and to gain some intuition concerning its dependence on various experimental parameters such as aperture radius and source wavelength. In the following sections, a brief overview of the theoretical background will be presented; this development will be followed by a comparison to the Kirchhoff results.

## 2. Theoretical Background

The basic assumptions of this approach should be emphasized. A single mode plane wave is assumed to be incident upon an infinitely thin screen with a perfectly circular aperture. The incident wave is aligned with the center of the aperture so that off-axis illumination is not considered in the following. This limitation is not an intrinsic difficulty so that the theory can be extended to include eccentricities of the circle (ellipses, for example) and off-axis illumination. Both types of boundary conditions are explicitly handled – the perfectly absorbing or perfectly reflecting conditions (Dirichlet or Neumann) on the screen. Non-ideal materials might be an unknown combination of these idealized boundaries. The treatment is limited to the scalar theory. A more complex numerical computation is required for the full vectorial solution.

The exact solution,  $u$ , can be generally expressed in terms of the integral equations

$$u = -\frac{1}{2\pi} \int \frac{\partial u}{\partial n} \frac{e^{ikr}}{r} d\Sigma, \quad (1)$$

and

$$u = \frac{1}{2\pi} \int u \frac{\partial}{\partial n} \left( \frac{e^{ikr}}{r} \right) d\Sigma, \quad (2)$$

where the integration is over the closed surface  $\Sigma$ . Denoting the Dirichlet solution as  $\phi_1$  so that  $\phi_1 = 0$  on the surface and the Neumann solution as  $\phi_2$  so that  $\frac{\partial \phi_2}{\partial n} = 0$  on the surface, the so-called Rayleigh equations for diffraction are

$$\phi_1 = \frac{1}{2\pi} \int_A \phi_1 \frac{\partial}{\partial n} \left( \frac{e^{ikr}}{r} \right) d\Sigma, \quad (3)$$

and

$$\phi_2 = -\frac{1}{2\pi} \int_A \frac{\partial \phi_2}{\partial n} \frac{e^{ikr}}{r} d\Sigma, \quad (4)$$

where the integration is now performed over the aperture  $A$  [3]. These equations are quite difficult to solve for an arbitrary aperture shape but some progress can be made for symmetric openings.

For problems with axial symmetry, a natural choice of co-ordinate system is oblate spheroidal co-ordinates [6]. Following Bouwkamp's terminology (which differs from

the standard definition [6]), the oblate spheroidal co-ordinates are designated as  $\xi, \eta,$  and  $\phi$  and are related to the cylindrical co-ordinates  $r, \phi,$  and  $z$  by

$$r/a = [(1 - \xi^2)(1 + \eta^2)]^{1/2} \quad (5)$$

$$z/a = \xi\eta \quad (6)$$

$$\phi = \phi \quad (7)$$

with the domains  $\eta \geq 0$  and  $-1 \leq \xi \leq 1$  where  $a$  is the radius of the aperture. The two unknown scalar waves can be expanded in a complete set of these functions

$$\phi_{1,2} = \sum_{n,m} \alpha_{nm} X_n^m(\xi) Y_n^m(\eta) e^{im\phi}, \quad (8)$$

where the  $\alpha_{nm}$  are the expansion coefficients, the  $X_n^m(\xi)$  are the "angular" spheroidal functions, and the  $Y_n^m(\eta)$  are the radial spheroidal functions. For circular apertures with on-axis illumination, there is no  $\phi$  dependence and the expansions are reduced to

$$\phi_{1,2} = \sum_n \alpha_n X_n(\xi) Y_n(\eta). \quad (9)$$

The integral equations, eqns. [3] and [4], can thus be reduced to the more numerically tractable differential equations where the expansion coefficients,  $\alpha_n$ , are determined by the boundary conditions. The most straightforward way to proceed, then, is to determine the "angular" spheroidal wave functions,  $X_n(\xi)$ , from their associated ordinary differential equation

$$(1 - \xi^2)X_n'' - 2\xi X_n' + (\lambda_n + k^2 a^2 \xi^2)X_n = 0 \quad (10)$$

which has the associated homogeneous Fredholm integral equation

$$X_n(\xi) = \mu_n \int_{-1}^1 \exp(ka\xi t) X(t) dt. \quad (11)$$

The quantity  $k$  is the wave number  $2\pi/\lambda$ . The normalization chosen corresponds to that of the Legendre polynomials in the limit  $ka = 0$

$$\int_{-1}^1 [X_n(\xi)]^2 d\xi = \frac{2}{2n+1}. \quad (12)$$

Although the "radial" wavefunctions,  $Y_n(\eta)$ , could also be found from their associated differential equation, a more convenient expression is

$$Y_n(\eta) = \frac{e^{ikan\eta}}{2} \int_{-1}^1 \frac{e^{-kat} X_n(t)}{i\eta - t} dt. \quad (13)$$

Thus once the angular functions are known, the radial solutions follow by a quadrature which is inherently more stable due to the smoothing effected by integration.

The two solutions,  $\phi_{1,2}$ , are now given by the expansions

$$\phi_1 = - \sum_{n=0}^{\infty} \frac{2(4n+3)\mu_{2n+1}}{ka + 2\pi i(\mu_{2n+1})^2} X_{2n+1}(\xi) Y_{2n+1}(\eta), \quad (14)$$

and

$$\phi_2 = \sum_{n=0}^{\infty} \frac{2(4n+1)\mu_{2n}}{ka + 2\pi i(\mu_{2n})^2} X_{2n}(\xi) Y_{2n}(\eta). \quad (15)$$

In the far-field limit,  $r \rightarrow \infty$ ,  $a\eta \approx r$  and  $\xi \approx \cos(\theta)$ , so that the general results approach the forms

$$\phi_1 \approx \frac{e^{ikr}}{ikr} \sum_{n=0}^{\infty} \frac{(4n+3)X_{2n+1}(1)}{1 + (2\pi i/ka)(\mu_{2n+1})^2} X_{2n+1}(\cos(\theta)), \quad (16)$$

and

$$\phi_2 \approx \frac{e^{ikr}}{ikr} \sum_{n=0}^{\infty} \frac{(4n+1)X_{2n}(1)}{1 - (2\pi i/ka)(\mu_{2n})^2} X_{2n}(\cos(\theta)). \quad (17)$$

These limiting forms explicitly display the exact deviations from sphericity. That is, these sums should be compared to the usual Kirchhoff approximation [1]

$$\phi_2 \approx \frac{e^{ikr}}{ikr} \frac{J_1(ka \sin(\theta))}{ka \sin(\theta)}, \quad (18)$$

where  $J_1(x)$  is a Bessel function of the first kind of order 1. It should be observed that the Kirchhoff expression is purely real except for the overall factor of  $\exp(ikr)$  - a feature not shared by the exact expression. This difference will have immediate consequences for the phase determination of the scattered wave.

Finally, transmission coefficients for the circular aperture can be derived

$$t_1 = \frac{4}{k^2 a^2} \sum_{n=0}^{\infty} \frac{(2n+3/2)[X_{2n+1}(1)]^2}{1 + (2\pi/ka)^2(\mu_{2n+1})^4} \quad (19)$$

and

$$t_2 = \frac{4}{k^2 a^2} \sum_{n=0}^{\infty} \frac{(2n+1/2)[X_{2n}(1)]^2}{1 + (2\pi/ka)^2(\mu_{2n})^4}. \quad (20)$$

These coefficients are useful as a verification of the numerical methods employed.

### 3. Numerical Results

The expansion technique described above was solved in the following manner. First, the angular wavefunctions were obtained by a relaxation method which simultaneously provides the characteristic values and their associated solutions on a grid for any given value of the dimensionless quantity  $ka$  and order  $n$  [7]. These values were extensively checked against tabulated values in those cases where comparisons existed [6]. The normalization of the angular functions was chosen to agree with Bouwkamp's description eqn [12]. Once these characteristic functions were obtained, the characteristic values,  $\mu_n$ , of the Fredholm equation eqn [11] were immediately calculated by a simple numerical quadrature. The radial function evaluation is likewise straightforward since it is also derived from the integral relation eqn [13].

As a check on the numerical procedure, the transmission coefficients, eqn [19] and eqn [20], were calculated and compared to those previously published [3] which were

obtained in a much more laborious fashion using recursion relations. The results of this comparison for a selected set of  $ka$  values are given in Table 1. In all cases the accuracy afforded by the numerical solution was high. The table entry for  $3\pi$  corresponds to the suggested value for the PDI which has  $a = 1.5\lambda$ .

Table 1  
Comparison of Transmission Coefficients.

$ka$	$t_1(exact)$	$t_1(Kirch)$	$t_2(exact)$	$t_2(Kirch)$
1.0	0.041061	0.0411	0.841502	0.8415
2.0	0.921772	0.922	0.917344	0.917
3.0	1.4179	1.42	0.976087	0.976
4.0	0.893444	0.893	0.987470	0.987
5.0	0.957660	0.958	0.987725	0.988
$3\pi$	1.02161		0.997258	

To assess the accuracy of the Kirchhoff approximation, a series of calculations were performed varying the quantity  $ka$  in the far-field,  $r = 150\lambda$ . This comparison was previously suggested by Spence [4]. The absolute value of the scalar wave solution is compared with that of the exact solution, eqn [15], as is the phase of the solution. For example, in figure 1 the amplitude for both the exact wavefunction and Kirchhoff approximation eqn [18] are plotted as a function of cylindrical angle in degrees for  $ka = 1$ . Although the qualitative dependence is reproduced by the approximation, it is not especially accurate. This comparison is continued in the following figures, 2 and 3, for  $ka = 2$  and 5 respectively. The Kirchhoff amplitude clearly improves as the aperture is enlarged for fixed wavelength. Figures 4 - 6 contain a comparison of the phase expected for the two solutions as a function of  $ka$ . In all cases the Kirchhoff approximation seriously misrepresents the phase of the scattered wave. In the experimentally interesting case of  $ka = 3\pi$ , a comparison of the two amplitudes is given in figure 7 and a comparison of the expected phases in figure 8.

Figure 1: Comparison of exact and approximate wave function amplitudes as a function of angle for  $ka = 1$ .

Figure 2: Amplitude comparison for  $ka = 2$ .

Figure 3: Amplitude comparison for  $ka = 5$ .

Figure 4: Comparison of exact and approximate wave function phases as a function of angle for  $ka = 1$ .

Figure 5: Phase comparison for  $ka = 2$ .

Figure 6: Phase comparison for  $ka = 5$ .

Figure 7: Comparison of exact and approximate wave function amplitudes as a function of angle for  $ka = 9.42478$  ( $3\pi$ ).

Figure 8: Comparison of exact and approximate wave function phases as a function of angle for  $ka = 9.42478$  ( $3\pi$ ).

Figure 9: Percent fractional error in the Kirchhoff approximation as a function of angle for  $ka = 9.42478$  ( $3\pi$ ).

The same pattern observed in the previous, lower  $ka$  value, plots reappears – the amplitude appears to match fairly well for all angles but the phase is only qualitatively reproduced. Although the amplitudes seem to match well for almost all angles, a plot of the percent deviation is given in figure 9. This deviation is defined by

$$Error = \frac{|\phi_{Exact} - \phi_K|}{\phi_{Exact}}, \quad (21)$$

where the subscripts denote the exact solution or the Kirchhoff approximation. A large fractional difference is obvious near those angles corresponding to phase changes (fringes). Thus, even for larger apertures the Kirchhoff approximation must be used with caution and is probably too unreliable for highly precise experiments.

Finally, an estimate of the deviation from sphericity expected in the far-field phase can be obtained from this scalar approach. The phase function was evaluated at  $0^\circ$  and  $20^\circ$  as a function of aperture radius to determine the departure of the phase from a constant value. These results are given in Table 2 with the maximum deviation given over this range of angles. The values from the scalar theory indicate that significant excursions from sphericity are expected as the aperture radius is increased.

Table 2

Phase differences, in degrees, expected at 0 and 20 degrees as a function of aperture radius,  $a$ .

$a(\lambda)$	$\phi(0^\circ)$	$\phi(20^\circ)$	maximum deviation
0.25	38.310	37.996	0.314
0.50	17.870	15.539	2.331
1.00	9.0574	2.4346	6.623
1.50	186.05	167.43	18.627
2.00	200.87	364.53	163.66

#### 4. Conclusions

A brief description of an exact scalar wave evaluation has been presented and compared to the well-known Kirchhoff approximation. The results essentially verify earlier predictions and calculations for selected cases. The comparison with published values is very favorable, indicating the accuracy and robustness of the numerical methodology. Some preliminary results describing the limitations of the Kirchhoff approach are given which emphasize the large discrepancies expected in the calculated phases of the scattered wave. This development can be extended to include off-axis illumination and non-zero eccentricities for the aperture. Likewise, an analogous extension of the calculational approach should be possible for the complete vector solution [8]. The technique cannot be used to determine the effect of a non-zero thickness of the screen and aperture. Similarly it is also physically limited to the scalar regime,  $ka > 1$ .

#### Acknowledgments

This work is performed under the auspices of the U. S. Department of Energy by the Lawrence Livermore National Laboratory under contract number W-7405-Eng-48.

#### References

- [1] E. Hecht, Optics, 2nd ed., Chp. 10, (Addison-Wesley, Reading MA, 1987).
- [2] J. D. Jackson, Classical Electrodynamics, 2nd edition, Chp. 9, (Wiley, New York, 1975).
- [3] C. J. Bouwkamp, "Diffraction Theory", Rep. Prog. Phys., ed. A. C. Stickland, vol. XVII, pp. 35-100, The Physical Society, London, 1954.
- [4] R. D. Spence, "The Diffraction of Sound by Circular Disks and Apertures", *J. Acous. Soc. Am.*, 20, 380-386(1948); R. D. Spence, "A Note on the Kirchhoff Approximation in Diffraction Theory", *ibid.*, 21, 98-100(1949).

- [5] G. Sommargren, Lawrence Livermore National Laboratory, (personal communication).
- [6] M. Abramowitz and I. Stegun, eds., Handbook of Matematical Functions, (NBS, Washington, D. C., 1972).
- [7] W. H. Press, Flannery, B. P. Flannery, S. A. Teulkosky, and W. T. Vetterling, Numerical Recipes, Sec 16.4, (Cambridge, London, 1986).
- [8] C. Flammer, "The Vector Wave Solution of the Diffraction of Electromagnetic Waves by Circular Disks and Apertures. II The Diffraction Problems", *J. Appl. Phys.*, **24**, 1224-1231(1953).

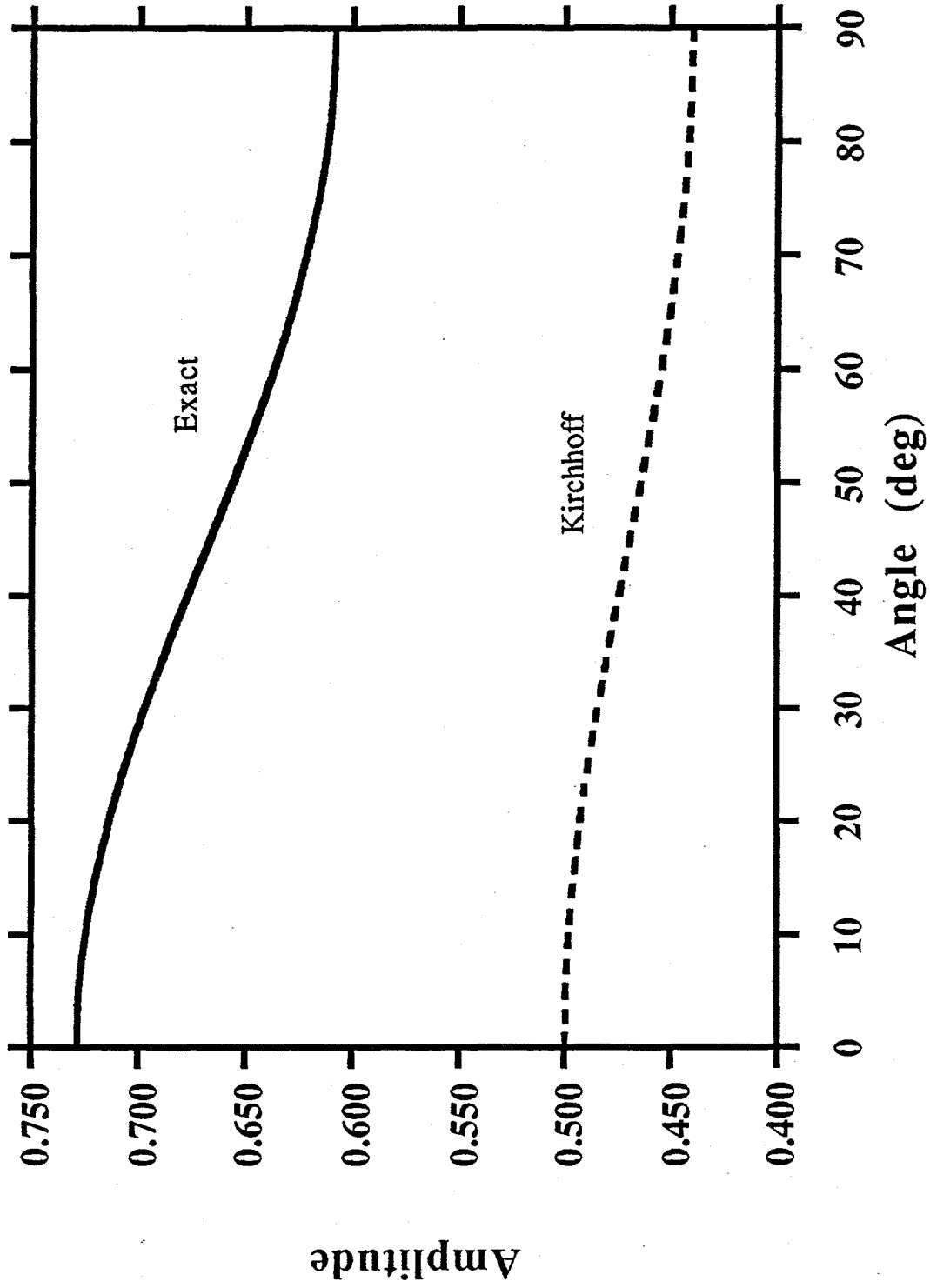


Figure 1

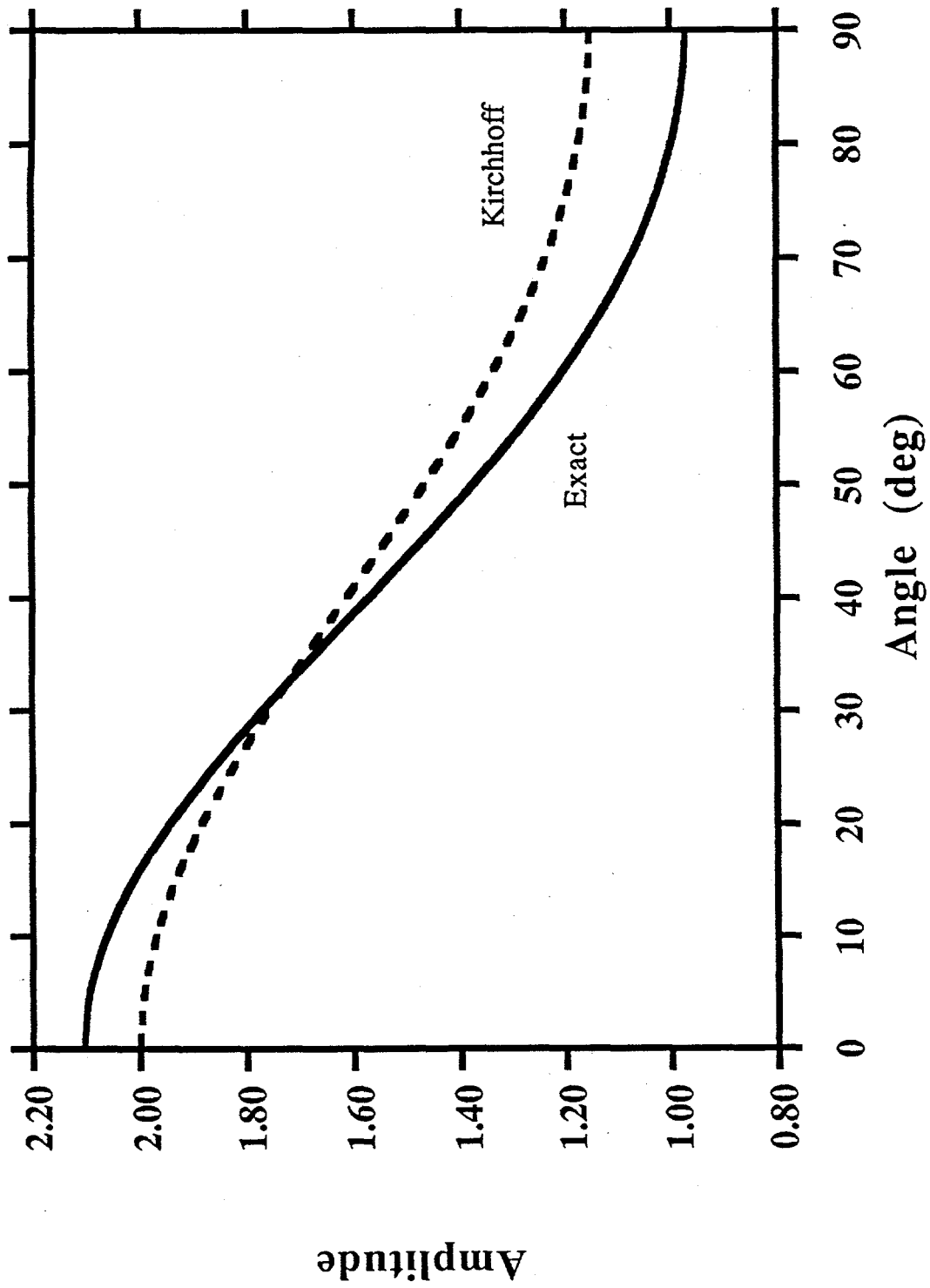


Figure 2

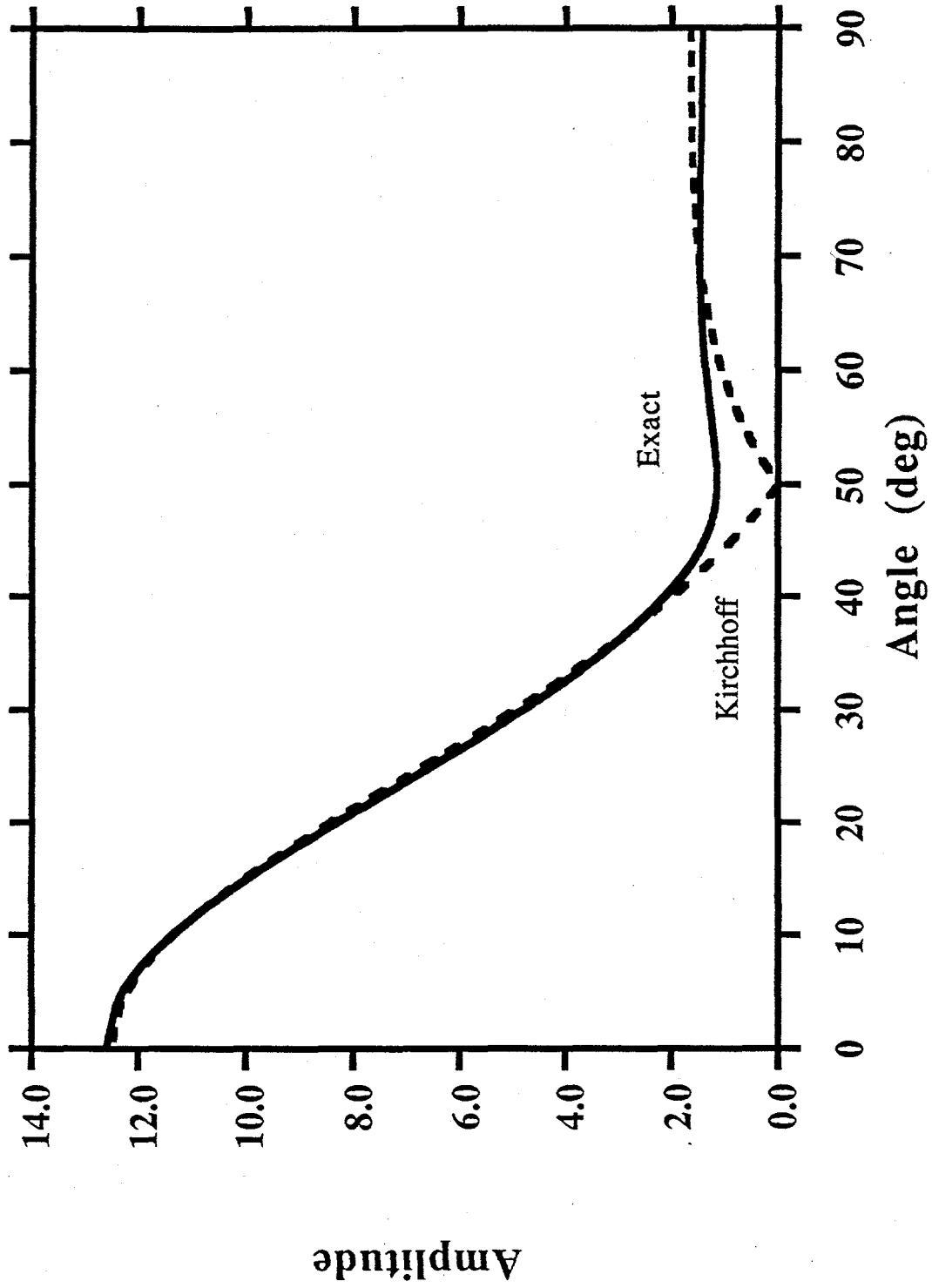


Figure 3

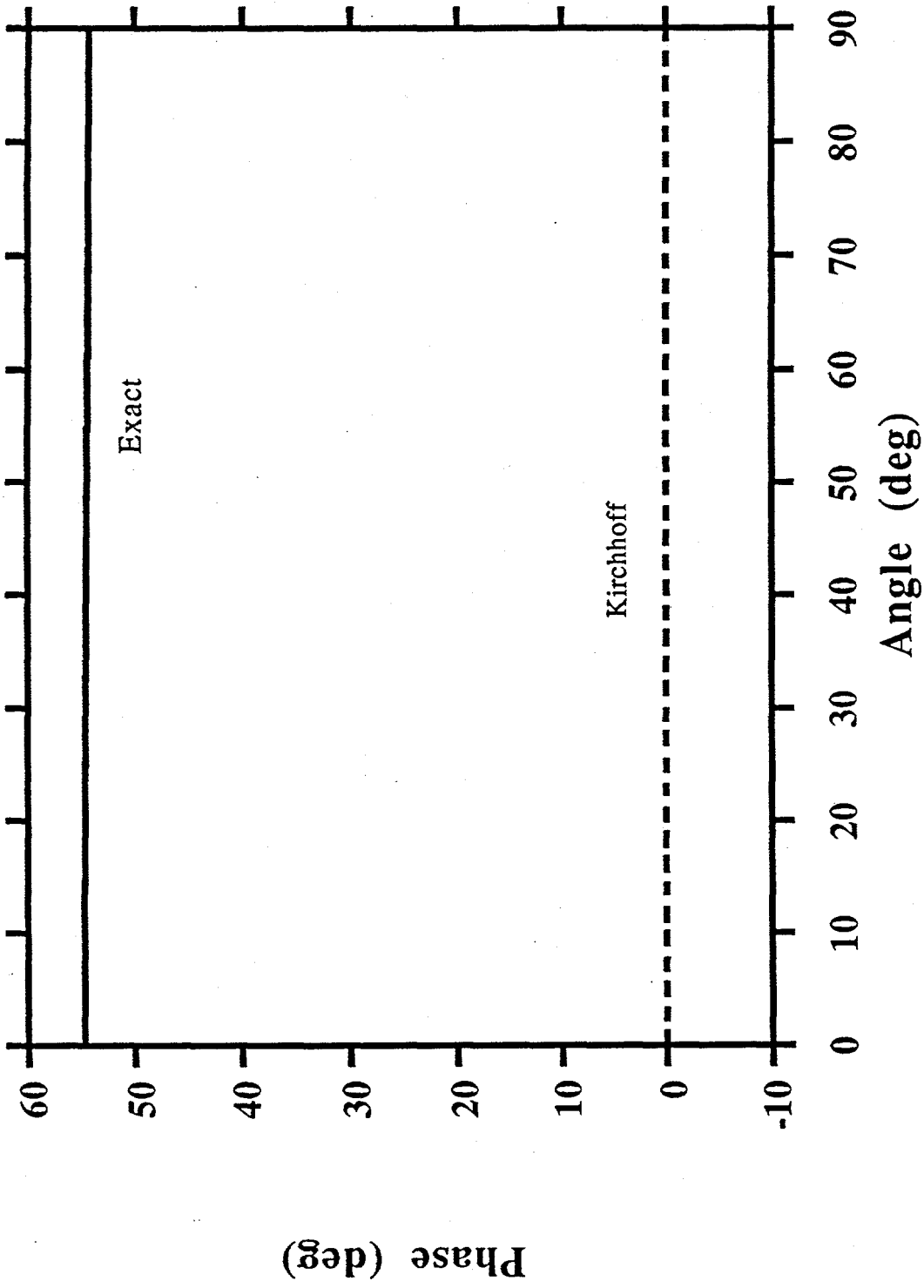


Figure 4

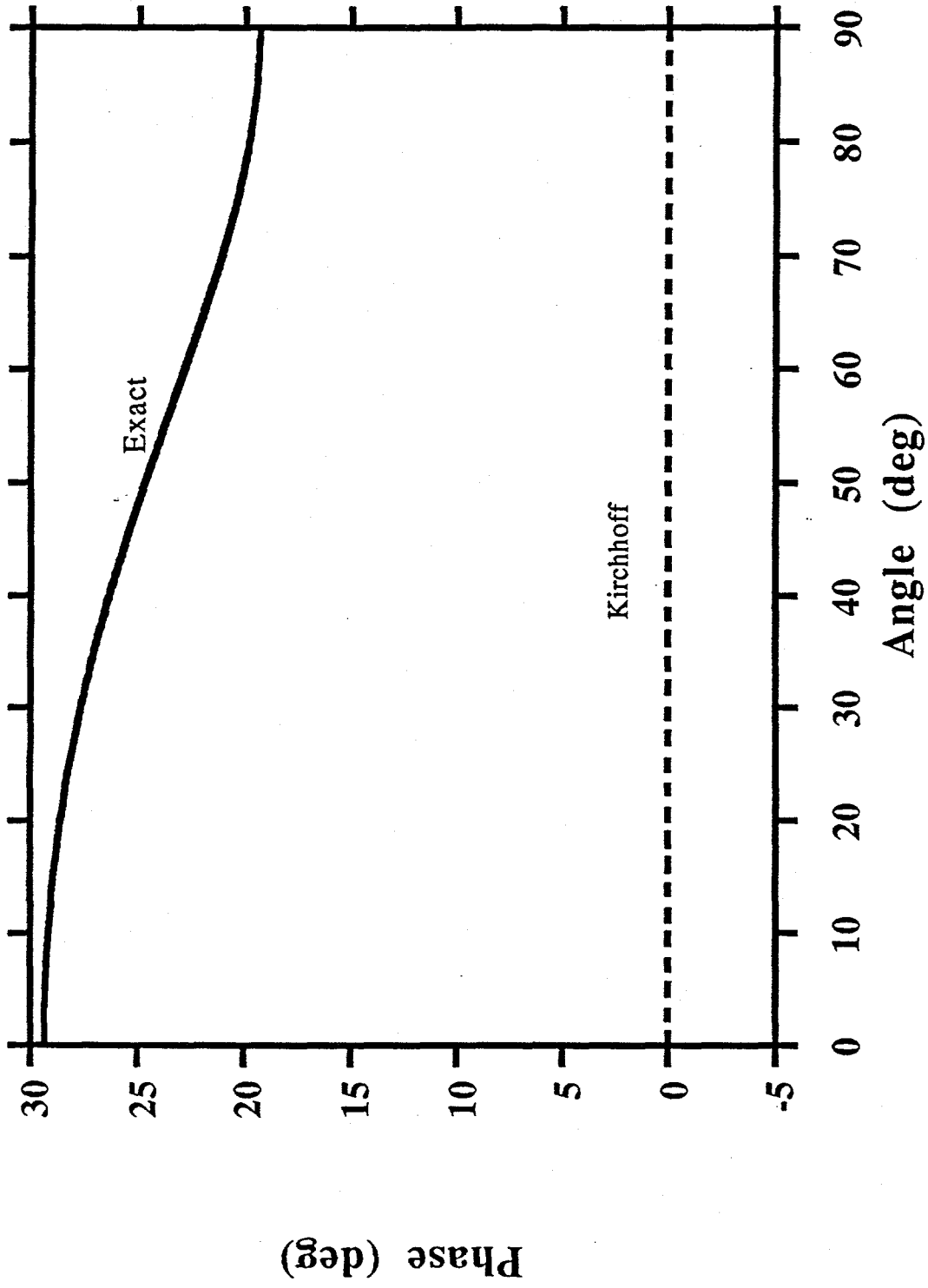


Figure 5

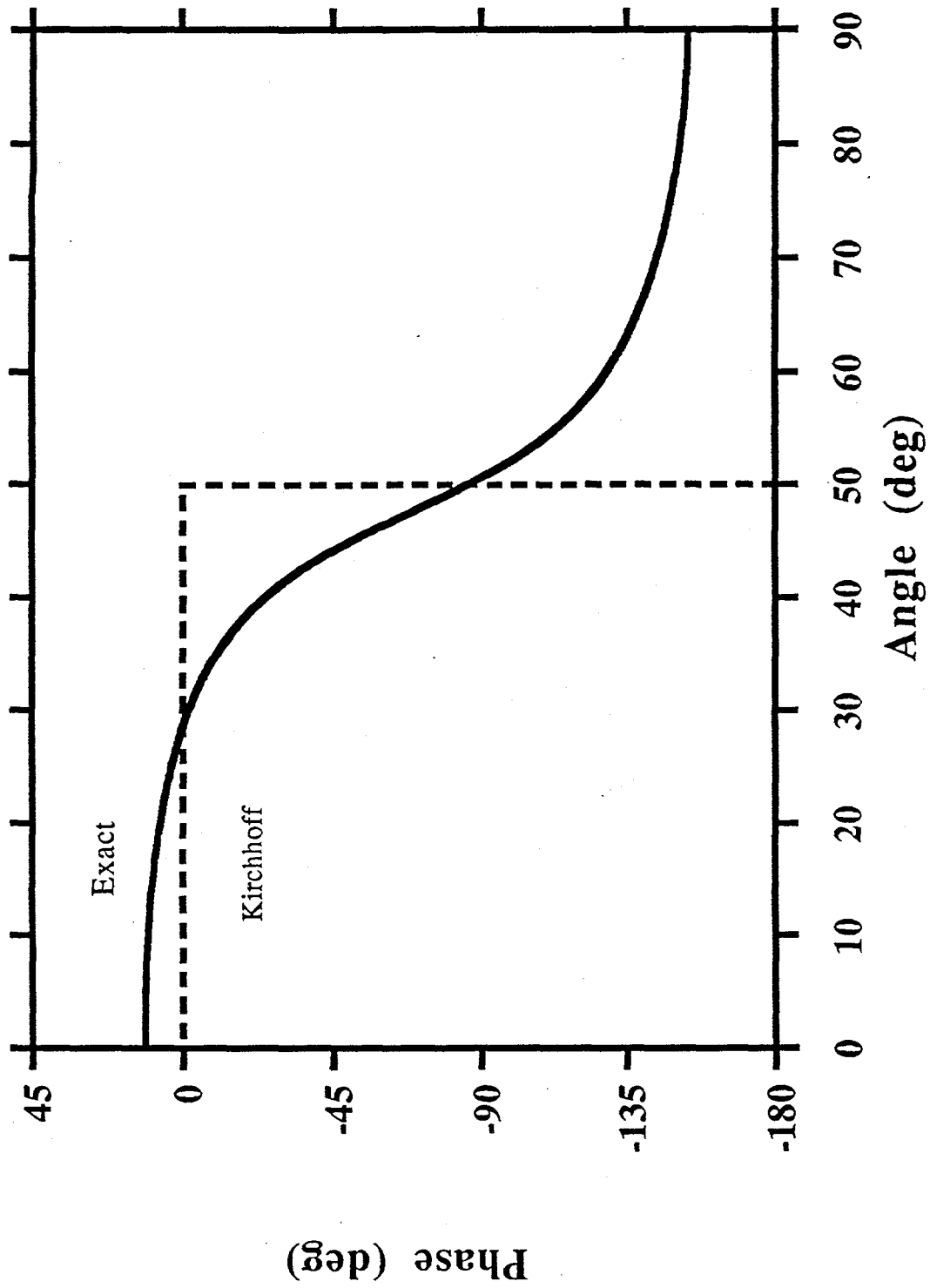


Figure 6

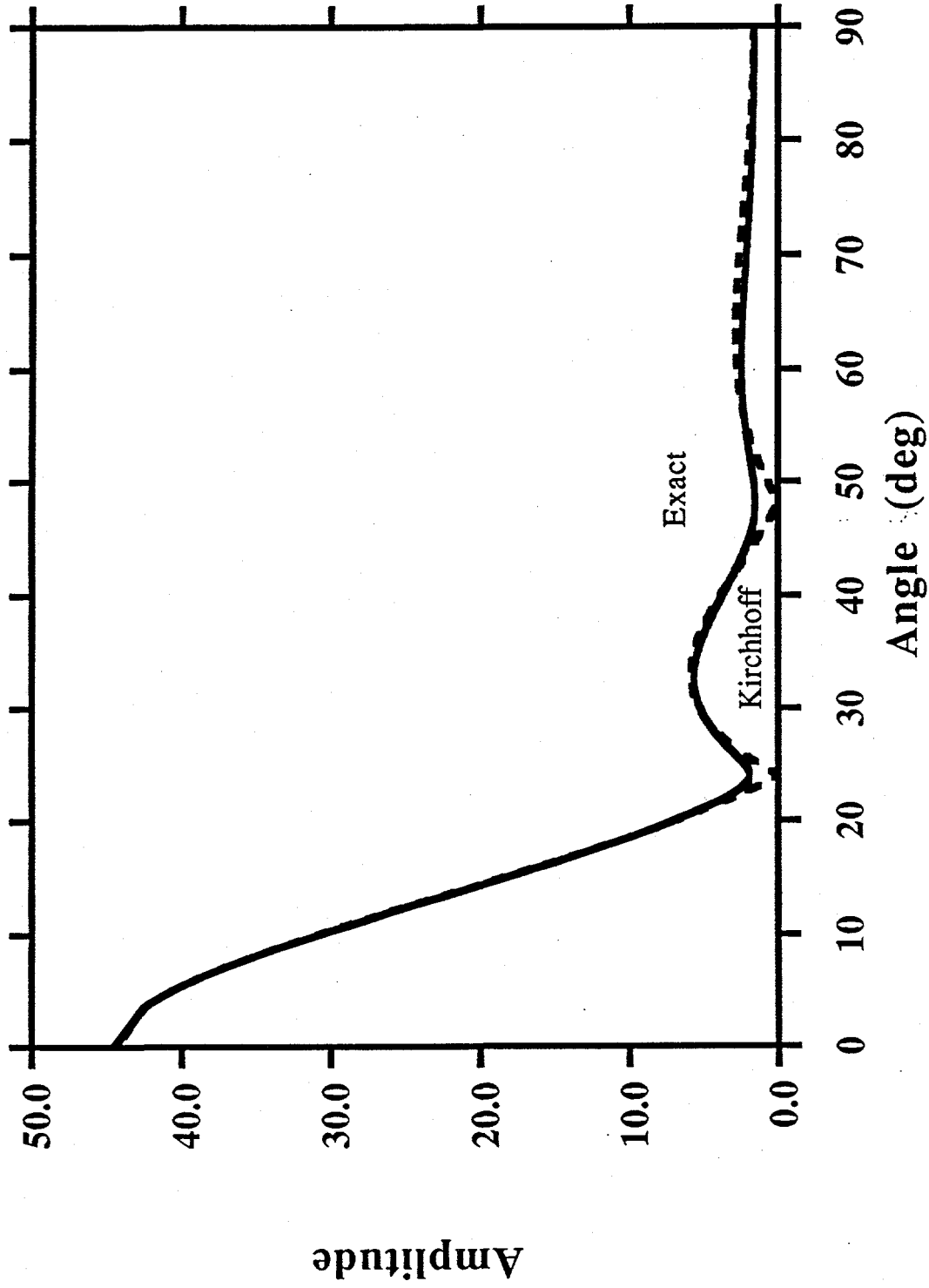


Figure 7

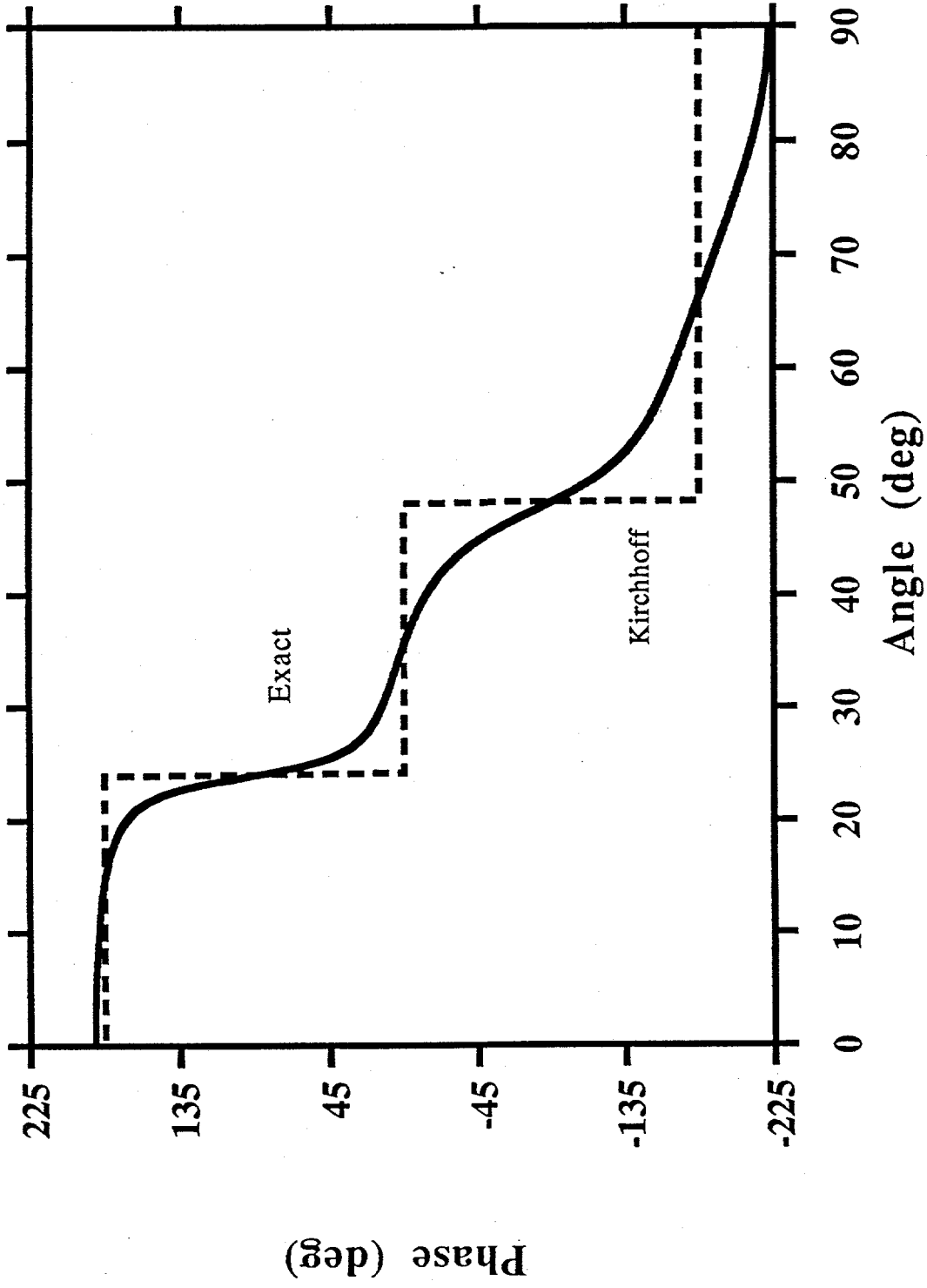


Figure 8

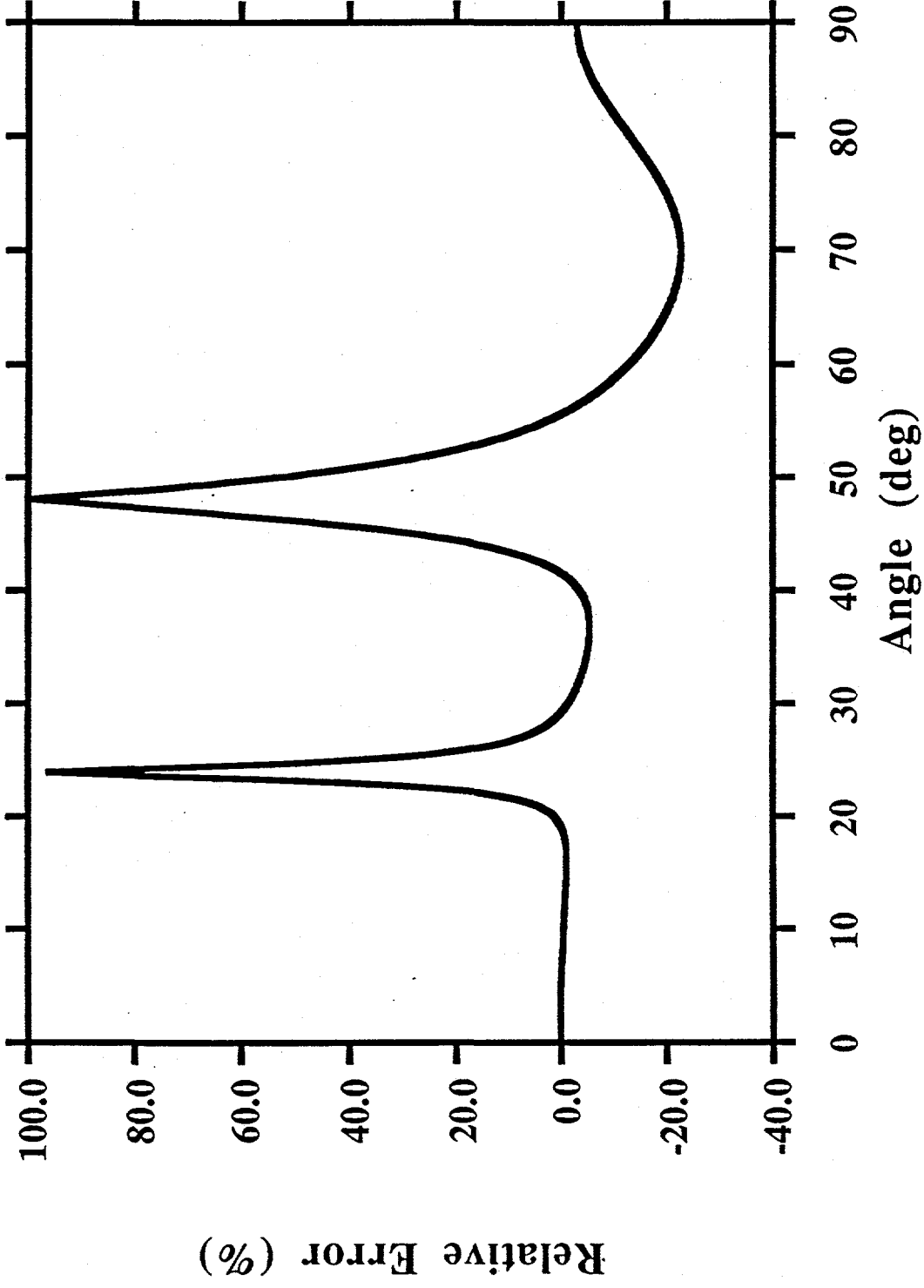


Figure 9